Journal of Engineering and Applied Sciences 13 (Special Issue 12): 9497-9502, 2018
ISSN: 1816-949X

Effect of in Addition on the Properties of CoCrMo (F75) Alloy Using P/M Technique

Hayder H.J. Jamal Al-Deen and Ekram A.R. Hassani
Department of Metallurgical Engineering, Faculty of Material Engineering,
University of Babylon, Babylon, Iraq

Abstract: This study investigates the effect of Indium addition on properties of CoCrMo (F75). The samples were prepared by powder metallurgy approach. The corrosion and wear behavior were investigated by using different tests, this tests including mechanical tests (hardness and wear) and electrochemical test (open circuit and potentiodynamic polarization). The results show that the addition of In caused decreasing in porosity. The hardness increases with in addition and the wear rate of F75 alloy decreases with the addition of In (In addition improves wear resistance), this decreasing in wear rate increases as the content of in increases. The corrosion of CoCrMo alloy was improved by the addition of In in both Hank's solution and artificial saliva.

Key words: CoCrMo alloy indium, powder metallurgy, wear, corrosion, resistance, saliva

INTRODUCTION

Implants are fabricated from a wide variety of materials including metals, polymers, ceramics and their composites. Among these materials, metals are an important group.

Stainless steel, Ti alloys and CoCrMo alloy are the common metals used in orthopedics applications (Walter, 2006). Cobalt chrome alloys are used widely for medical prosthesis implant devices because they have a great biocompatibility and spontaneous chromite formation of a passive layer which provides the material high corrosion resistance. They are used where high stiffness or highly polished and extremely wear resistant material is required. The cobalt chrome alloys are the main choice for many surgical applications such as knee implant, metal to metal hip joints and dental implants (Jacobs *et al*., 1998).

Indium was discovered by Feerdinand Reich and Hieronymons Theodor Richter by spectroscopic methods. It is a post-transition metal that make up 0.21 part per million of the crust of the Earth (Haynes, 2010). The physical appearance is a white silvery, high ductile post-transition metal a bright luster (Alfantazi and Moskalyk, 2003).

This research highlights to improve the mechanical and electrochemical properties of F75 alloy by addition different percentages of Indium (A1 = 0.5, A2 = 1, A3 = 1.5, A4 = 2% and M master alloy).

MATERIALS AND METHODS

The materials powders used to prepare (F75) CoCrMo alloy are listed in Table 1 and 2 with average particle size (measured by using Better size 2000 laser particles size analyzer), purity (by handheld XRF analyzer) and chemical composition of F75 alloy.

The weighted powders have been wetly mixed by using planetary automatic ball mill, steel balls with different diameter have been used and Ethanol has been added as a mixing medium of wet mixing. The mixing process was being carried out for 5 h.

Table 1: Purity and average particle size of materials

Materials	Purity (%)	Average particle size (μm)	Chemical composition (%)
Chrome	99.95	41.480	28
Molybdenum	99.90	12.760	6
Nickel	99.44	43.260	2.5
Iron	99.78	59.340	0.75
Carbon	99.44	37.440	0.35
Silicon	99.11	51.470	1
Manganese	99.39	52.310	1
Indium	99.99	40.150	(0.5, 1, 1.5 and 2)
Cobalt	99.95	6.464	Balance

Table 2: Alloy code and composition

Alloy code	Composition (%)
M	F75
A1	F75+0.5
A2	F75+1.0
A3	F75+1.5
A4	F75+2.0

Corresponding Author: Hayder H.J. Jamal Al-deen, Department of Metallurgical Engineering, Faculty of Material Engineering, University of Babylon , Babylon, Iraq

Table 3: Chemical composition of etching solution

Constituents	Values (mL)
HNO_3	15
Acetic Acid	15
HCl	60
Water	15

Powder mixture has been compacted by using electric hydraulic press to produce a disk sample with dimension of 12.8 mm in diameter and 3 mm thickness, the compacting pressure was 800 MPa and holding time was 2 min. Graphite used as a lubricant to reduce the friction during the pressing process. The sintering process has been carried out under vacuum conditions by using vacuum tube furnace.

The samples of sintering process include the following steps: heating from room temperature to 500°C, soaking for 2 h at 500°C, heating from temperature 500-950°C, soaking for 5 h at 850°C, slow cooling in the furnace with continues vacuum circumstances to the room temperature.

Microstructure: All samples after sintering process were grinded by using (180, 400, 600, 800, 1000, 1200, 1500, 2000) grit silicon carbide papers, then polished with a diamond past of 15 μm to get a bright mirror finish for the final step.

Etching was made at room temperature, Table 3 illustrated the chemical composition of the etching solution (Odahara *et al*., 2008). After etching process the samples were washed with water and dried. The porosity of sintered samples is calculated according to (Anonymous, 2003).

Macohardness: Macrohardness Brinell tester is used to measure the hardness of the samples with 31.25 kg/mm^2 as applying weight and the incubation time was 10 sec in state applied weight and diameter 2.5 mm.

Dry sliding wear test: The wear test had been covered according to ASTM G 99 (Hemza, 2013).

$$\text{Wear rate} = (\text{Weight loss g})/(\text{Density g/cm}^3) \quad (1)$$

Electrochemical test: The corrosive behavior of CoCrMo studied in two different solutions (artificial saliva and Hank's solution). The pH of artificial saliva and Hank's solution at 37°C were 6.7 and 7.4, respectively. The chemical composition of both solutions is shown in Table 4 and 5 (Dawood, 2014).

Table 4: Chemical composition of artificial saliva

Constituent	Values (g/L)
KCl	1.5
$NaHCO_3$	1.5
$NaH_2PO_4H_2O$	0.5
HSCN	0.5
Lactic acid	0.9

Table 5: Chemical composition of Hank's solution

Constituent	Values (g/L)
NaCl	8.00
$CaCl_2$	0.14
KCl	0.40
$NaHCO_3$	0.35
Glucose	1.00
$MgCl_2 6H_2O$	0.10
$Na_2HPO_4.H_2O$	0.06
KH_2PO_4	0.06
$MgSO_4.7H_2O$	0.06

Open Circuit Potential (OCP): The tests were carried out with the samples immersed in a Hank's solution and artificial saliva. The potential of the working electrode is measured with respect to a Saturated Calomel Electrode (SCE).

Potentiodynamic polarization: Electrochemical experiments were performed in three electrode cell containing and electrolytes similar to nature saliva and Hank's solution. The counter electrode was Pt and the reference electrode was SCE and working electrode (specimen) according to the American Society for Testing and Materials (ASTM). The test was conducted by stepping the potential using a scanning rate 0.4 mV/s from initial potential of 350 mV below the open circuit potential and the scan continued up to 350 mV above the open circuit potential. Corrosion rate measurement is obtained by using the following equation (Jaber, 2014):

$$\text{Corrosion rate} = (0.13I_{corr}.EW)/\rho \quad (2)$$

RESULTS AND DISCUSSION

The porosity of all sintered alloys was measured, Fig. 1 show the effect of In on the porosity of sintered samples, there is a decreasing in the porosity values after sintering process. The porosity decreasing with increasing in content. There is a significant rising in the hardness values with addition of in Fig. 2 and 3 shows the effect of in content on the hardness, the hardness increasing with increasing adding percentage and the cause of this rising is related to the change of microstructure morphology induced by in addition. All samples with 12.8 mm are subjected to wear test under various loads (10, 15 and 20) N for different time (5, 10, 15, 20 and 25) min at room temperature (Fig. 4-8).

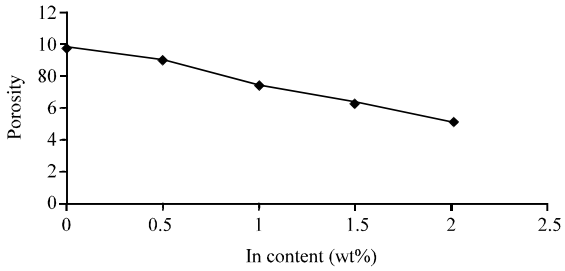

Fig. 1: Effect of In content on the porosity for alloys (M, A1-A4)

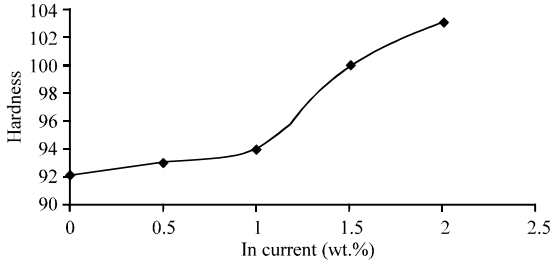

Fig. 2: Effect of In addition on the hardness for M, A1-A4

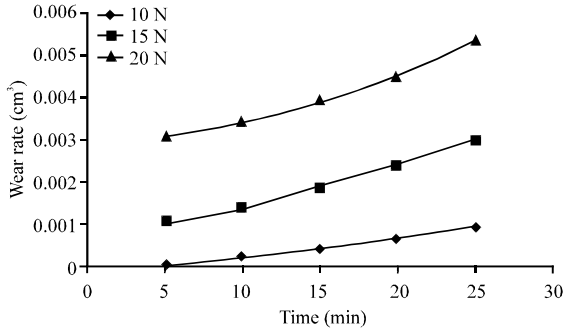

Fig. 3: Wear rate vs. time for M alloy

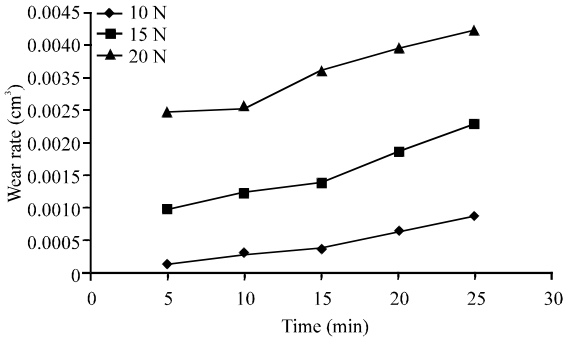

Fig. 4: Wear rate vs. time for A1 alloy

From Fig. 9 which shows the effect of in content on wear rate of A1-A4 under constant load (20 N) and constant time (25 min), it can be noted that the

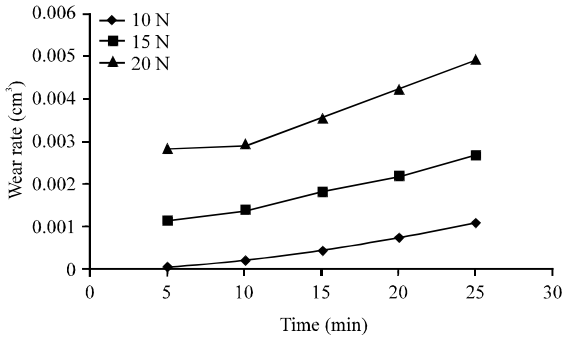

Fig. 5: Wear rate vs. time for A2 alloy

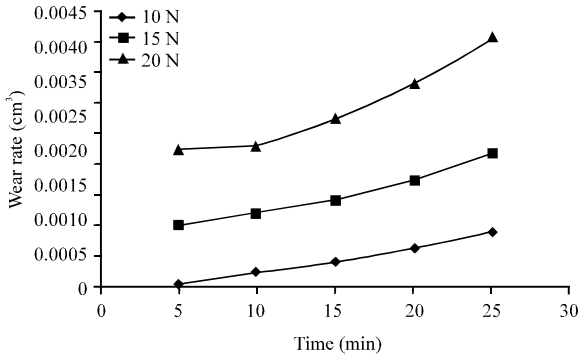

Fig. 6: Wear rate vs. time for A3 alloy

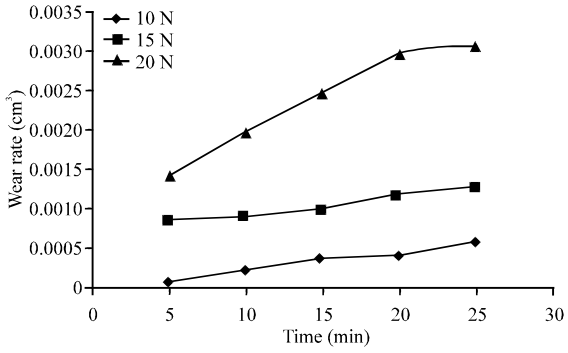

Fig. 7: Wear rate vs. time for A4 alloy

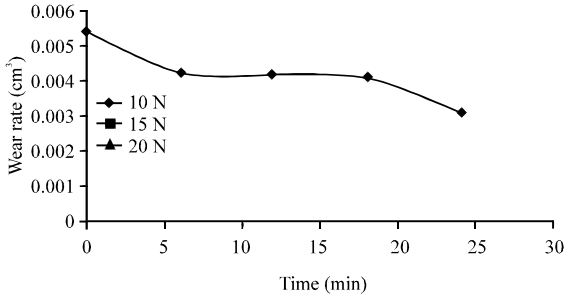

Fig. 8: Effect of In on wear rate at 20 N and 25 min

Table 6: Corrosion current (Icorr.), corrosion potential (Ecorr.) and corrosion rate for all alloys in Hank's solution at 37±1°C

Alloy	Icorr. (μA/cm^2)	Ecorr. (mV)	Corrosion rate (mpy)	Improvement (%)
M	8.26	-432.3	3.152	--
A1	6.35	-431.2	2.407	23.63
A2	6.11	-428.7	2.324	26.26
A3	5.90	-422.6	2.258	28.36
A4	5.20	-385.4	1.992	36.80

Table 7: Corrosion current (Icorr.), corrosion potential (Ecorr.) and corrosion rate for all alloys in artificial saliva at 37±1°C

Alloy	Icorr. (μA/cm^2)	Ecorr. (mV)	Corrosion rate (mpy)	Improvement (%)
M	3.83	-435.5	1.462	--
A1	2.24	-384.2	0.849	41.92
A2	2.19	-375.3	0.836	42.82
A3	0.74	-370.8	0.283	80.64
A4	0.678	-350.4	0.259	82.28

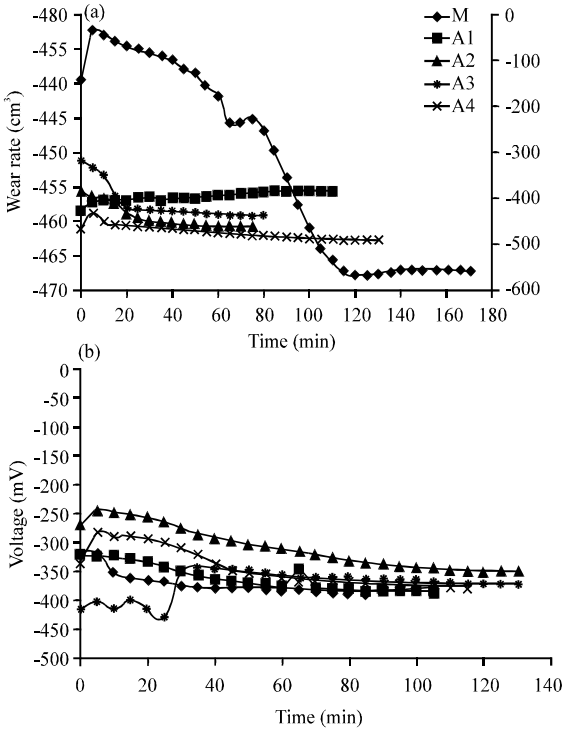

Fig. 9: OCP- time; a) In Hank's solution and b) In artificial saliva

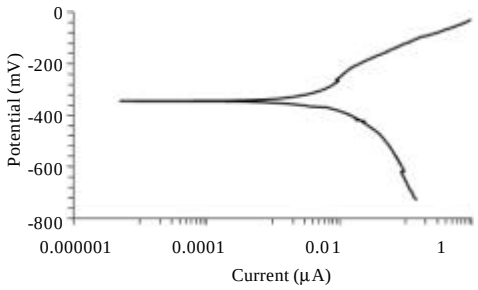

Fig. 10: Potentiodynamic polarization for M alloy in Hank's solution

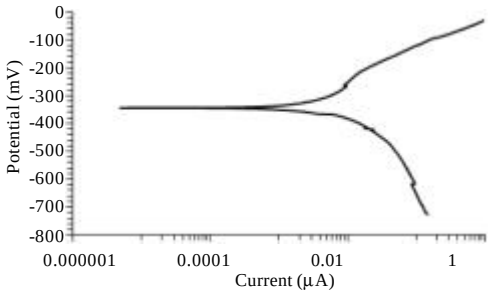

Fig. 11: Potentiodynamic polarization for M alloy in artificial saliva

wear rate decreasing with increasing in content, this reduction in wear rate return to in addition which increases hardness and reduces porosity.

Electrochemical tests

Open Circuit Potential (OCP)-time measurement: The OCP time was measured for all alloys in Hank's solution and artificial saliva at 37±1°C, Fig. 10 shows the evolution of corrosion potential of the alloys through time. The time period was from 0-170 min with interval of 5 min were potentially reported.

From Fig. 10, it can be noted that during 25-30 min the corrosion potential increases at greatest speed, this because the formation of metal oxide on the surface, then the corrosion potential increases slowly because the growth of oxide film which improving corrosion protection ability. Also, it can be noted that the corrosion potential reaches a level at which the corrosion potential stabilize. The constant OCP means that there is equilibrium between dissolution and deposition (Fig. 10-16).

From Table 6 it can be noted that there is a significant improvements in corrosion resistance of F75 alloys with different additives of in (0.5, 1, 1.5 and 2) wt.%, Icorr. for samples is ranged from (6.35 μA/cm^2) for A1 alloy to (5.20 μA/cm^2) for A4 alloy which are lower than Icorr. for M alloy which is (8.26 μA/cm$_2$) and Ecorr. for A alloys is ranged from (-431.2 mV) for A1 alloy to (-385.4 mV) for A4 alloy which are higher than Ecorr. for M alloy which is (-432.3 mV) in Hank's solution.

From Table 7, it can be noted that there is an improvement in corrosion resistance of CoCrMo alloy with different additives of In (0.5, 1, 1.5 and 2) wt.% in artificial saliva, Icorr. for A alloys is graded from (2.24 μA/cm^2) for A1 alloy to (0.678 μA/cm^2) for A4 alloy

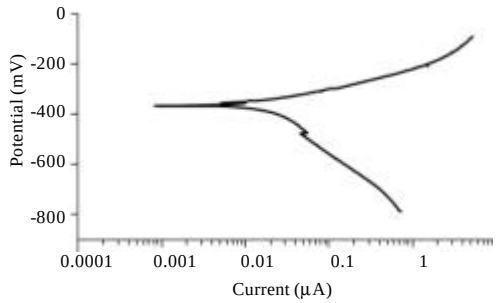

Fig. 12: Potentiodynamic polarization for A4 alloy in Hank's Solution

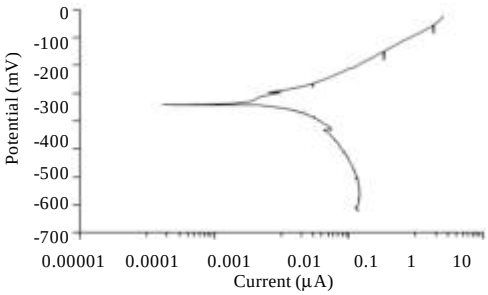

Fig. 13: Potentiodynamic polarization for A4 alloy in artificial saliva

which are lower than Icorr. for M alloy which is (3.83 µA/cm^2) and Ecorr. for A alloys is graded from (-384.2 mV) for A1 alloy to (-350.4 mV) for A4 alloy which are higher than Ecorr. for M alloy which is (-435.5). From data listed in Table 6 and 7, it can be seen that the corrosion current of CoCrMo alloy with in addition is lower than CoCrMo alloy in Hank's solution and artificial saliva. This is because of that in element enhances corrosion resistance of CoCrMo alloy by formation of passive film.

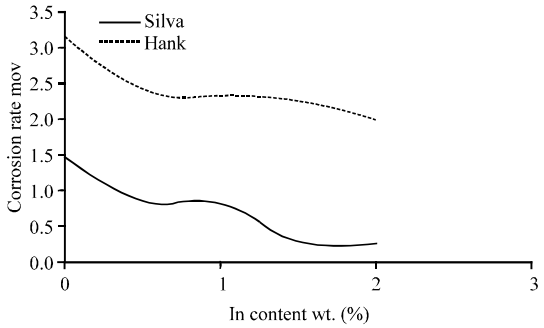

Fig. 14: Effect of In content on the corrosion rate of M, A1-A4 alloys in Hank's solution and artificial saliva at 37±1°C

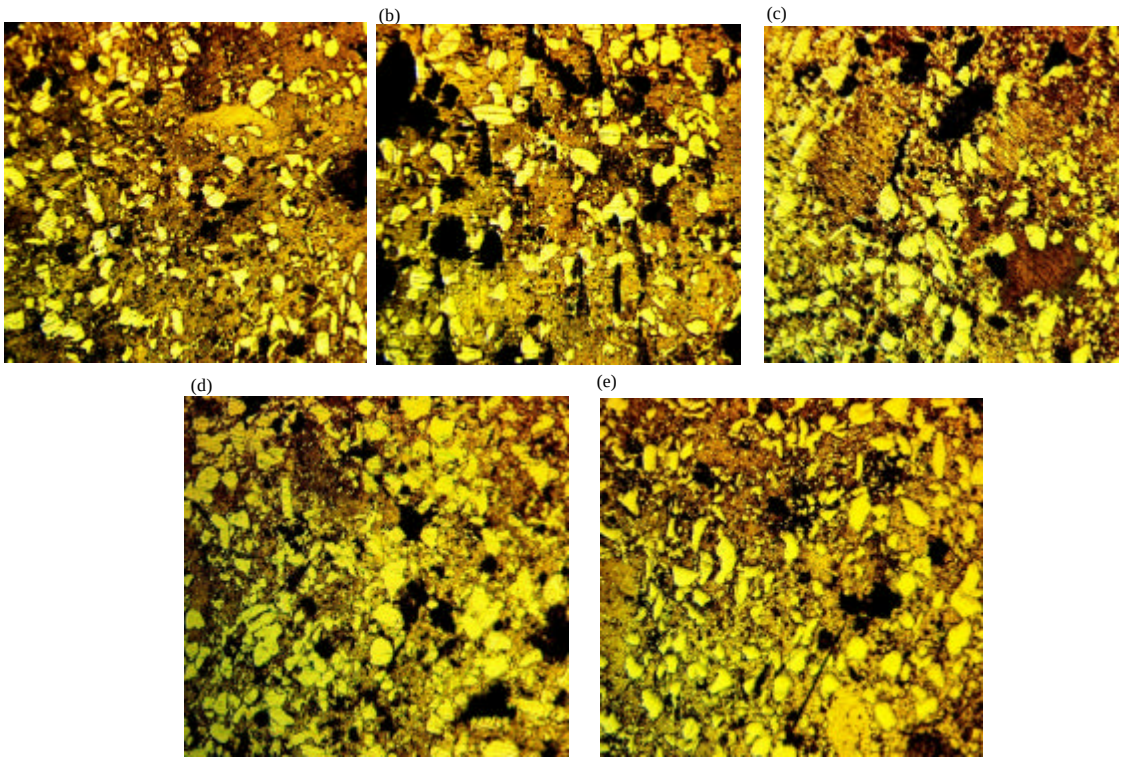

Fig. 15a-c: Microstructure for M, A1-A4 alloys after sintering process

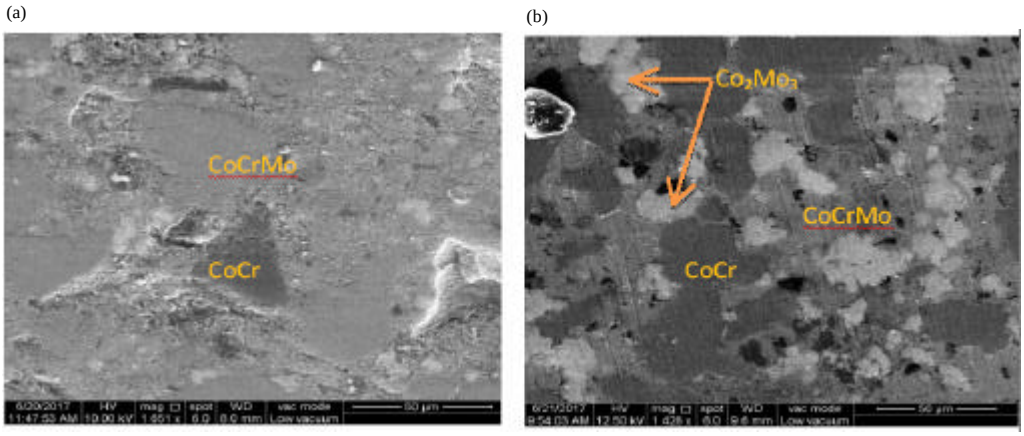

Fig. 16a-c: SEM images for etched M and A4 alloy with 50 μm magnification

The corrosion rate decreases with increasing In content for all samples in tow corrode solutions as shown in Fig. 15.

CONCLUSION

The addition of In to CoCrMo alloys leads to decreasing porosity and increasing hardness. The wear resistance increased with the addition of in and it's increasing with increasing in content. The corrosion resistance of F75 alloy improved with in addition in Hank's solution and artificial saliva and it's increasing with increasing In content. The Icorr. for used alloys in artificial saliva is lower than that in Hank's solution.

REFERENCES

Alfantazi, A.M. and R.R. Moskalyk, 2003. Processing of indium: A review. Miner. Eng., 16: 687-694.

Anonymous, 2003. 328, Standard test method for density, oil content and interconnected porosity of sintered metal structural parts and oil-impregnated bearing. ASTM International, West Conshohocken, Pennsylvania, USA.

Dawood, N.M., 2014. Preparation and characterization of bio nitinol with addition of copper. Ph.D Thesis, Materials Engineering Department, University of Technology, Baghdad, Iraq.

Haynes, W.M., 2010. CRC Handbook of Chemistry and Physics: A Ready-Reference Book of Chemical and Physical Data. CRC Press, Boca Raton, Florida, USA.,.

Hemza, A.S., 2013. Study of microstructure, corrosion and dry sliding wear of copper aluminum-nickel shape memory alloys. MSc Thesis, University of Babylon, Hillah, Iraq.

Jaber, H.H., 2014. The effect of admixed Ti on corrosion resistance of high copper dental amalgam. J. Babylon Univ. Eng. Sci., 22: 413-421.

Jacobs, J.J., J.L. Gilbert and R.M. Urban, 1998. Corrosion of metal orthopaedic implants. J. Bone Joint Surg., 80: 268-282.

Odahara, T., H. Matsumoto and A. Chiba, 2008. Mechanical properties of biomedical Co-33Cr-5Mo-0.3 N alloy at elevated temperatures. Mater. Trans., 49: 1963-1969.

Walter, M., 2006. Benefits of P/M processed cobalt-based alloy for orthopaedic medical implants. Carpenter Technology Corp., Wyomissing, Pennsylvania, USA.